Molecular Therapy
Oncolytics
Original Article

Overexpression of YBX1 Promotes Pancreatic Ductal Adenocarcinoma Growth via the GSK3B/Cyclin D1/Cyclin E1 Pathway

Zhiqiang Liu,[1,3] Yongfeng Li,[2,3] Xiaogang Li,[1] Jingyuan Zhao,[1] Shihong Wu,[1] Heshui Wu,[1] and Shanmiao Gou[1]

[1]Department of Pancreatic Surgery, Union Hospital, Tongji Medical College, Huazhong University of Science and Technology, Wuhan 430022, China; [2]Department of Gastrointestinal Surgery, Union Hospital, Tongji Medical College, Huazhong University of Science and Technology, Wuhan 430022, China

Pancreatic ductal adenocarcinoma (PDAC) is among the most lethal cancers due to frequently late diagnosis and futile treatment. It is a crucial necessity to determine the mechanisms of PDAC. Y-box Binding Protein 1 (YBX1), a highly conserved transcription factor, has been previously reported to play a role in various hallmarks of cancer. We show here that YBX1 is significantly overexpressed in PDAC and correlates with poor prognosis and reduced survival. In PDAC cell lines, YBX1 regulated cell-cycle progression, proliferation, and the expression of glycogen synthase kinase 3 beta (GSK3B) and cell-cycle-related proteins cyclin D1 and E1. Dual-luciferase reporter and chromatin immunoprecipitation (ChIP) assays established that YBX1 binds to the promoter of *GSK3B*, suggesting that YBX1 promotes pancreatic cancer cell growth through induction of GSK3B expression. These findings offer important insights into the mechanisms underlying pathologic proliferation in PDAC.

INTRODUCTION

Pancreatic ductal adenocarcinoma (PDAC) is one of the most lethal cancers due to frequently late diagnosis and futile treatments.[1,2] PDAC accounted for approximately 3% of new cancer diagnoses in 2017 in the United States and was responsible for more than 7% of US deaths from all types of cancer.[3] Conventional treatment approaches have had little impact on the course of this aggressive cancer. The 5-year survival rate of pancreatic cancer is about 8%, which remains similar to that of 30 years ago.[4] Thus, it is vital to determine the mechanisms of PDAC in order to develop further treatment strategies.

Y-box Binding Protein 1 (YBX1), a highly conserved transcription factor, regulates transcription and translation as a multi-functional DNA/RNA binding protein. YBX1 modulates gene transcription through binding in a cell-type-specific manner to promoters that harbor Y-box motifs.[5] YBX1 was previously reported to play a role in various hallmarks of cancer.[5] YBX1 performs its functions both in the cytoplasm and nucleus. It could not only bind to the enhancers of *EGFR* (epidermal growth factor receptor) and *erbB2* (HER2) genes, but also could secrete through the non-canonical pathways, activating the signal transduction. Ladomery and Sommerville[6] found that YBX1 also played an important role in regulating cell proliferation and embryonic development. YBX1 was involved in DNA damage repairing, RNA splicing, multidrug resistance, and cancer progression as a transcriptional factor or independent of transcriptional factor.[7] We show here that YBX1 is overexpressed and inversely correlated with prognosis in PDAC. Further, YBX1 binding to the *GSK3B* promoter triggers GSK3B transcription, thereby promoting cyclin D1/E1 expression. The cell proliferation and G1 cell-cycle arrest induced by YBX1 overexpression can be reversed by GSK3B knockdown. Here we provided an apparent mechanism for further amplifying GSK3B expression and activity in PDAC.

RESULTS

YBX1 Is Elevated in PDAC and Is Associated with Poor Outcome

To explore the relationship between YBX1 and malignancy of PDAC, we first examined expression levels of total YBX1 in PDAC and matched paracancer specimens by immunohistochemical (IHC) analysis. The randomly selected IHC staining images were demonstrated in Figure 1A. YBX1 protein expression was higher in PDAC tissues than in matched paracancer tissues (Figure 1B). Only 13.3% of matched paracancer tissues (12 of 90) displayed positive expression of YBX1; the remaining 86.7% of paracancer tissues (78 of 90) were negative for YBX1 expression (Figure 1C). However, 72.2% of the cancer tissues (65 of 90) were positive for YBX1 expression (Figure 1C). This is consistent with the previous study.[8]

The datasets containing 178 cases revealed markedly higher *YBX1* transcript expression in PDAC compared with normal pancreatic tissues in GEO (Figure 1D). Moreover, the data from the datasets

Received 9 February 2020; accepted 20 March 2020;
https://doi.org/10.1016/j.omto.2020.03.006.

[3]These authors contributed equally to this work.

Correspondence: Shanmiao Gou, PhD, Department of Pancreatic Surgery, Union Hospital, Tongji Medical College, Huazhong University of Science and Technology, Wuhan 430022, China.
E-mail: shanmiaogou@hust.edu.cn
Correspondence: Heshui Wu, PhD, MD, Department of Pancreatic Surgery, Union Hospital, Tongji Medical College, Huazhong University of Science and Technology, Wuhan 430022, China.
E-mail: heshuiwu@hust.edu.cn

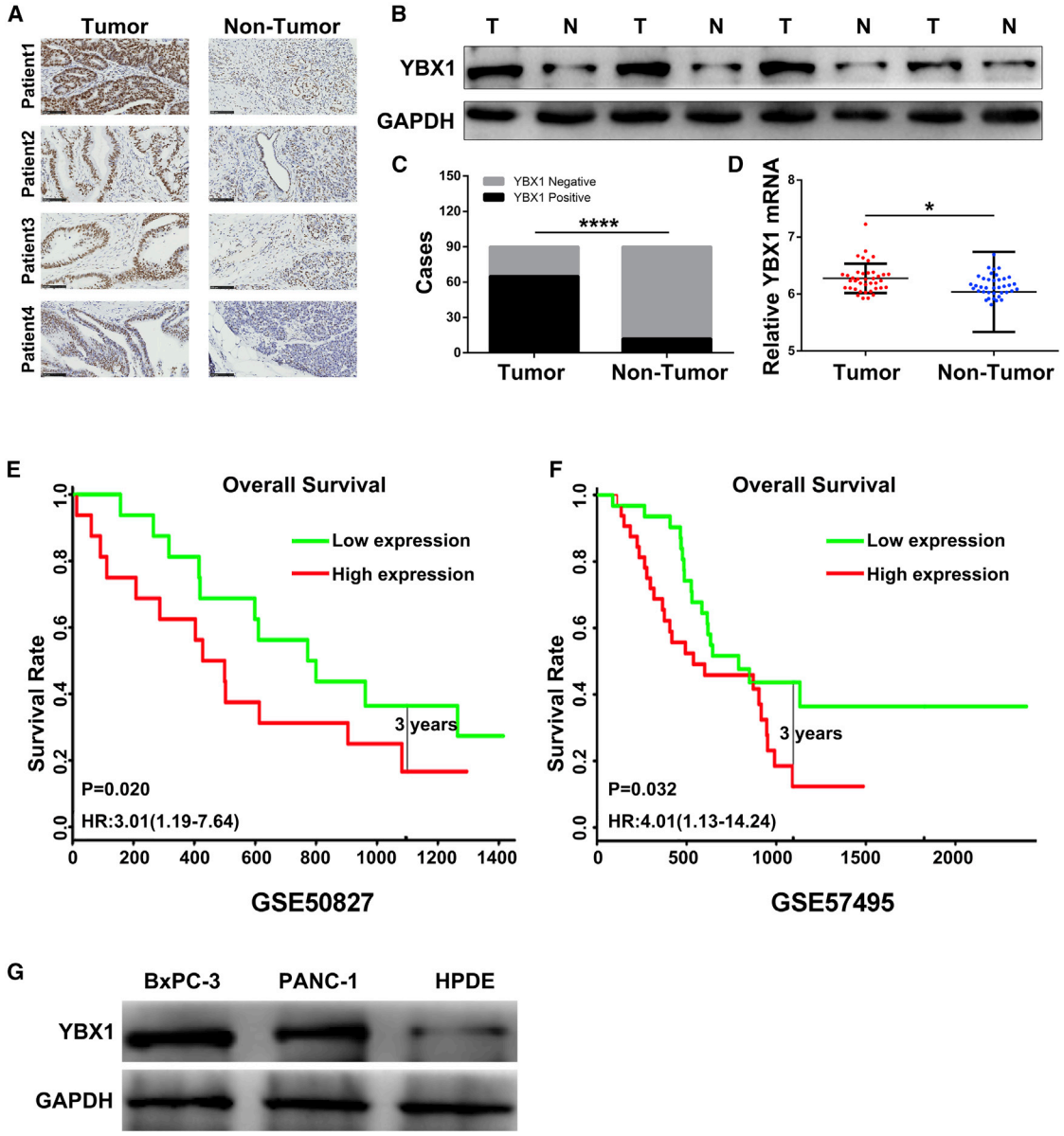

Figure 1. YBX1 Is Elevated in PDAC and Is Associated with Poor Outcome

(A) Randomly selected images of YBX1 immunostaining in pancreatic cancer and normal pancreatic tissues. Strong YBX1 staining is detected in primary PDAC tissue; YBX1 showed no or weak staining in adjacent noncancerous tissues. (B) The YBX1 protein levels were examined by western blot in cancer and paracancer tissues. (C) The positive rate of specimens with YBX1 expression is analyzed. The columns represent cancerous tissues and paracancerous tissues. (D) The *YBX1* mRNA expression profiles are collected from the datasets GEO: GSE22780, GSE15471, GSE16515, and GSE32676 (https://www.ncbi.nlm.nih.gov/geo/). The datasets had been analyzed using the Affymetrix HG-U133 Plus 2.0 platform (GPL570), which included 70 normal pancreatic specimens and 108 PDAC specimens. We used log2 transformation (normalized count) for the analysis. (E) The *YBX1* mRNA expression profiles are collected in human and normal human pancreas based on The Cancer Genome Atlas (TCGA) data and the Genotype-Tissue Expression (GTEx) project in GEPIA (http://gepia.cancer-pku.cn/). (F) Effect of YB1 expression level on PDAC patient overall survival (OS). The mRNA sequencing (mRNA-seq) data for PDAC were downloaded from TCGA Research Network (https://www.cancer.gov/about-nci/organization/ccg/research/structural-genomics/tcga). Both clinical and mRNA-seq data were retrieved from the datasets. The data were processed by edgeR package of R language. OS was analyzed between groups with low and high *YBX1* mRNA expression in PDAC patients via GraphPad Prisma 6. *YBX1* mRNA expression was significantly negatively correlated with patient OS rate. (G) The levels of YBX1 protein expression are assessed by western blot analyses in one normal pancreatic ductal epithelial cell line, HPED, and two pancreatic cancer cell lines, BxPC-3 and PANC-1. Error bars indicate standard deviation. Kaplan-Meier curves were analyzed by log rank tests. The t test was used to compare the difference between groups. *$p < 0.05$; **$p < 0.01$; ***$p < 0.001$; ****$p < 0.0001$.

GEO: GSE50827 and GSE57495 showed that elevated *YBX1* expression also significantly correlates with poor overall survival in PDAC (Figures 1E and 1F).

In addition, YBX1 protein expression levels in HPNE (representing normal pancreatic ductal epithelial tissue), high YBX1 expression in PDAC cell line BxPC-3, and relatively low YBX1 expression in PDAC cell line PANC-1 were analyzed using immunoblotting. In agreement with the above results, substantially higher levels of YBX1 expression were observed in PDAC cell lines (Figure 1G). Altogether, these results demonstrate that YBX1 expression is elevated in PDAC and is correlated with poor outcome.

YBX1 Knockdown Inhibited Cell Proliferation, Cell-Cycle Progression, Cell-Cycle-Related Proteins, and GSK3B in PDAC Cells

To explore the role of YBX1 in cell proliferation, we silenced YBX1 in BxPC-3 and PANC-1 using two short hairpin RNAs (shRNAs), designated here as shRNA1 and shRNA2. Both of the YBX1-specific shRNAs efficiently suppressed expression levels of *YBX1* mRNA and YBX1 protein compared with the scrambled control shRNA (Figures 2A and 2B). Under the same conditions, cell growth was significantly inhibited by transfection of YBX1-silencing shRNAs compared with the control shRNA (Figures 2C and 2D). Gene set enrichment analysis (GSEA) of YBX1 revealed that the Kyoto Encyclopedia of Genes and Genomes (KEGG) cell-cycle pathway was enriched in the high YBX1 group (Figures 2E and 2F).

In addition, YBX1 knockdown led to a significant increase in the proportion of cells in G1 phase and a decrease in the proportion of cells in S phase in both cell lines (Figures 3A and 3B).

Our previous study found that GSK3B regulates cell growth in PDAC.[9] Accordingly, we found that *YBX1* mRNA levels positively correlated with *GSK3B* mRNA levels in Gene Expression Profiling Interactive Analysis (GEPIA) (Figure 3C).[10] PCR and western analysis revealed that YBX1 knockdown was also associated with a decrease in expression of GSK3B (Figures 3D and 3E). To address the mechanisms responsible for the proliferation inhibition by YBX1 silencing, we analyzed the cell-cycle regulators cyclin D1 and cyclin E1. We found that downregulation of YBX1 remarkably decreased the protein expression of cyclin D1 and cyclin E1 (Figure 3E).

Overexpression of YBX1 Regulates Cell Proliferation through GSK3B

To establish the relationship between YBX1 and cell-cycle-related proteins, we re-assessed the expression levels of these target molecules after overexpression of YBX1 (Figures 4A–4C). Western analysis showed that upregulation of YBX1 enhanced basal expression of GSK3B, cyclin D1, and cyclin E1 (Figure 4C). YBX1 overexpression also decreased the proportion of cells in G1, increased S phase proportion (Figures 4D and 4E), and significantly increased cell proliferation (Figures 4F and 4G). Interestingly, upon GSK3B knockdown, we observed that the effects mediated by YBX1 overexpression were all reversed (Figures 4D–4H).

In vivo, YBX1-overexpressing cells formed larger tumors and grew faster than the control group in nude mice (Figures 5A and 5B), and the tendency was also reversed by GSK3B silencing (Figures 5A and 5B). Moreover, western analysis and IHC staining of the tumors confirmed the results we demonstrated *in vitro* (Figures 5C–5E). Taken together, these results imply that YBX1 may regulate cell proliferation through GSK3B.

YBX1 Binds to the Promoter of *GSK3B*

We scanned a 2-kb genomic region upstream of the *GSK3B* transcriptional start site (http://www.genome.ucsc.edu/), and based on the transcriptional factor target prediction bioinformatic software, we identified three YBX1 binging sites, including one site including putative Y box sequences 5′-TGATTGGCCAC-3′ (Figure 6A), which have previously been identified as DNA binding sites for YBX1.[11,12] To elucidate whether YBX1 regulates the promoter activity of *GSK3B*, we conducted luciferase assays using a *GSK3B* reporter plasmid (Figure 6B). Luciferase activity in BxPC-3 cells cotransfected with a YBX1 expression vector was almost 2-fold higher than in cells transfected with empty vector (Figure 6B). Furthermore, depletion of YBX1 in BxPC-3 cells suppressed *GSK3B* promoter activity (Figure 6B). These results indicate that YBX1 positively regulates *GSK3B* promoter activity.

To determine whether YBX1 directly binds to the *GSK3B* promoter, we performed chromatin immunoprecipitation (ChIP) assays in BxPC-3 cells. A schematic representation of the potential YBX1 binding region within the *GSK3B* promoter and the locations of primers used for the ChIP assay are shown in Figure 6A. Three primer sets encompassing three YBX1 binding sites across the 2-kb promoter region of interest were used: "Y1" (−151 to −355 bp relative to the transcription start site), "Y2" (−321 to −426 bp), and "Y3" (−470 to −666 bp). As shown in Figure 6A, endogenous YBX1 in BxPC-3 cells bound the promoter of *GSK3B* within the "Y2" genomic interval. Semiquantitative evaluation is also shown in Figure 6C. Because depletion of YBX1 by shRNA eliminated detection of an immunoprecipitated DNA fragment from the "Y2" region, we conclude that "Y2" is the specific binding region for YBX1 in the *GSK3B* promoter.

In summary, these results suggest that YBX1 binds to the GSK3B promoter near the transcription start site and promotes transcription of GSK3B, increasing GSK3B protein levels and inducing cell-cycle arrest and cell proliferation in PDAC cells.

DISCUSSION

YBX1 is a transcription factor with cell-type-specific regulation.[5] The link between YBX1 upregulation and cancer cell growth has been established in some cancers,[13,14] but the impact of YBX1 on the biological processes and mechanisms in PDAC has been rarely studied. Here, we provide evidence that YBX1 is elevated in PDAC and is correlated with poor prognosis. We further documented that YBX1 binds to the *GSK3B* promoter, activating *GSK3B* transcription in

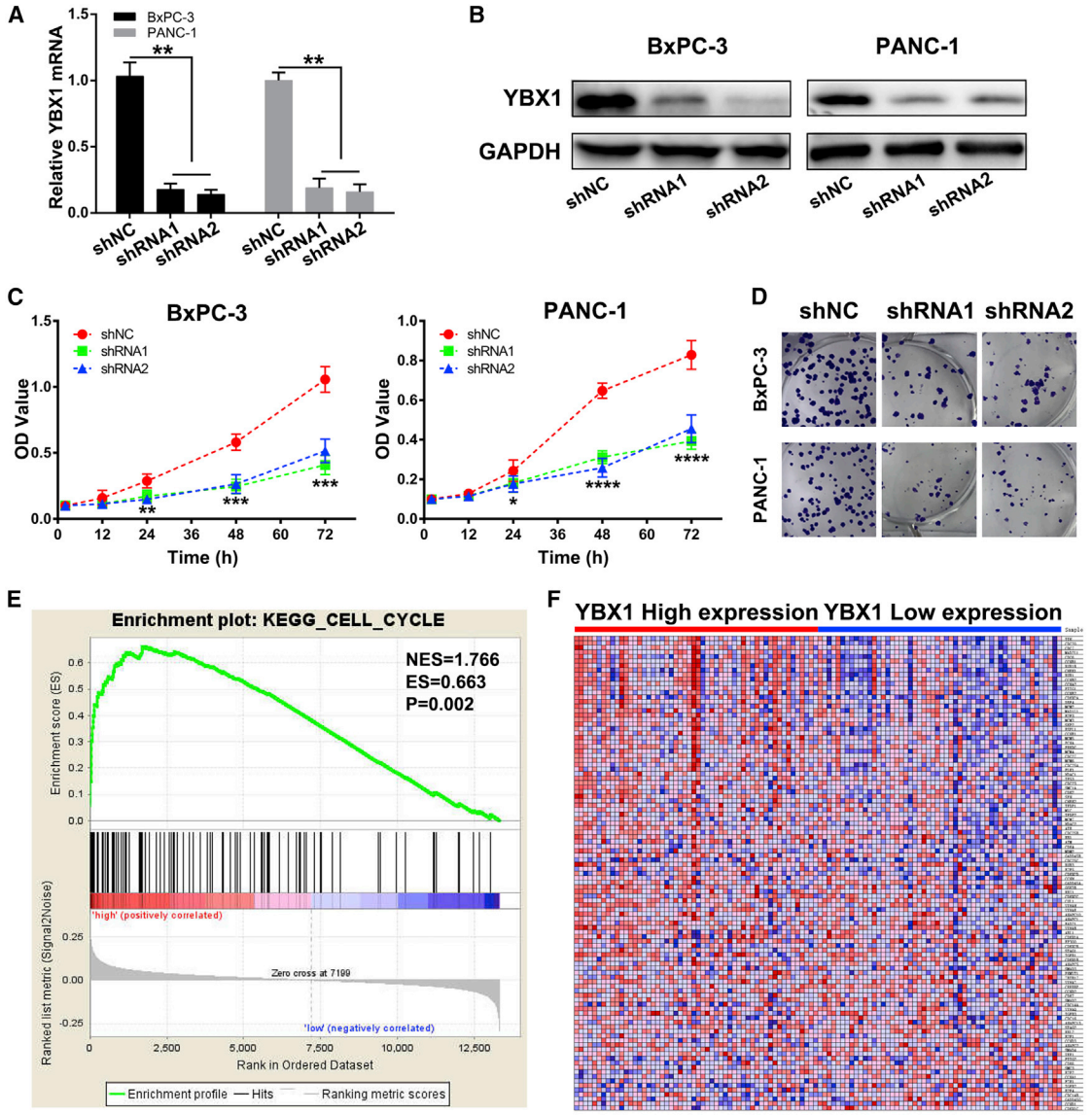

Figure 2. YBX1 Knockdown Reduces Cell Proliferation in PDAC Cells, and the KEGG Cell-Cycle Pathway Is Enriched in the High YBX1 Group

(A) The expression levels of *YBX1* mRNA. The pancreatic cancer cells were transfected with YBX1 shRNA lentiviral vectors to knock down *YBX1* gene expression. The expression levels of *YBX1* mRNA were assessed in BxPC-3 and PANC-1. The expression levels of *YBX1* mRNA were significantly lower in the YBX1 shRNA1- or shRNA2-transfected groups compared with the control group in BxPC-3 and PANC-1. (B) YBX1 proteins were assessed in BxPC-3 and PANC-1. YBX1 proteins were significantly lower in the YBX1 shRNA1- or shRNA2-transfected groups compared with the control group in BxPC-3 and PANC-1. (C) Silencing YBX1 in BxPC-3 and PANC-1 inhibited cell proliferation. PDAC cells treated with shRNA1, shRNA2, or control shRNAs were cultured for 12, 24, 48, and 72 h; CCK-8 assay was conducted for cell proliferation analysis. Cell proliferation was significantly lower in the YBX1 shRNA1- or shRNA2-transfected groups compared with the control group. (D) Cell proliferation was assessed by colony formation. (E) Enrichment of genes by GSEA. The *YBX1* mRNA expression profiles are collected from the datasets GEO: GSE22780, GSE15471, GSE16515, and GSE32676. We used log2 transformation (normalized count) for the analysis. The gene group with high *YBX1* mRNA was enriched in the KEGG cell-cycle pathway. (F) Heatmap of core enrichment genes in the gene set KEGG cell-cycle pathway. Error bars indicate standard deviation. The *t* test was used to compare the difference between groups. *$p < 0.05$; **$p < 0.01$; ***$p < 0.001$; ****$p < 0.0001$.

pancreatic adenocarcinoma cells. GSK3B upregulates cyclins D1 and E1, and promotes cell growth in pancreatic adenocarcinoma cells.

YBX1 is a broadly studied transcription factor, and it has been previously reported to play a role in various hallmarks of cancer.[5] We previously showed that GSK3B signaling is aberrantly activated and is associated with malignant biological behavior in PDAC. A further pairwise gene correlation analysis using gene expression datasets from The Cancer Genome Atlas (TCGA) and/or the Genotype-Tissue Expression (GTEx) project in GEPIA showed that

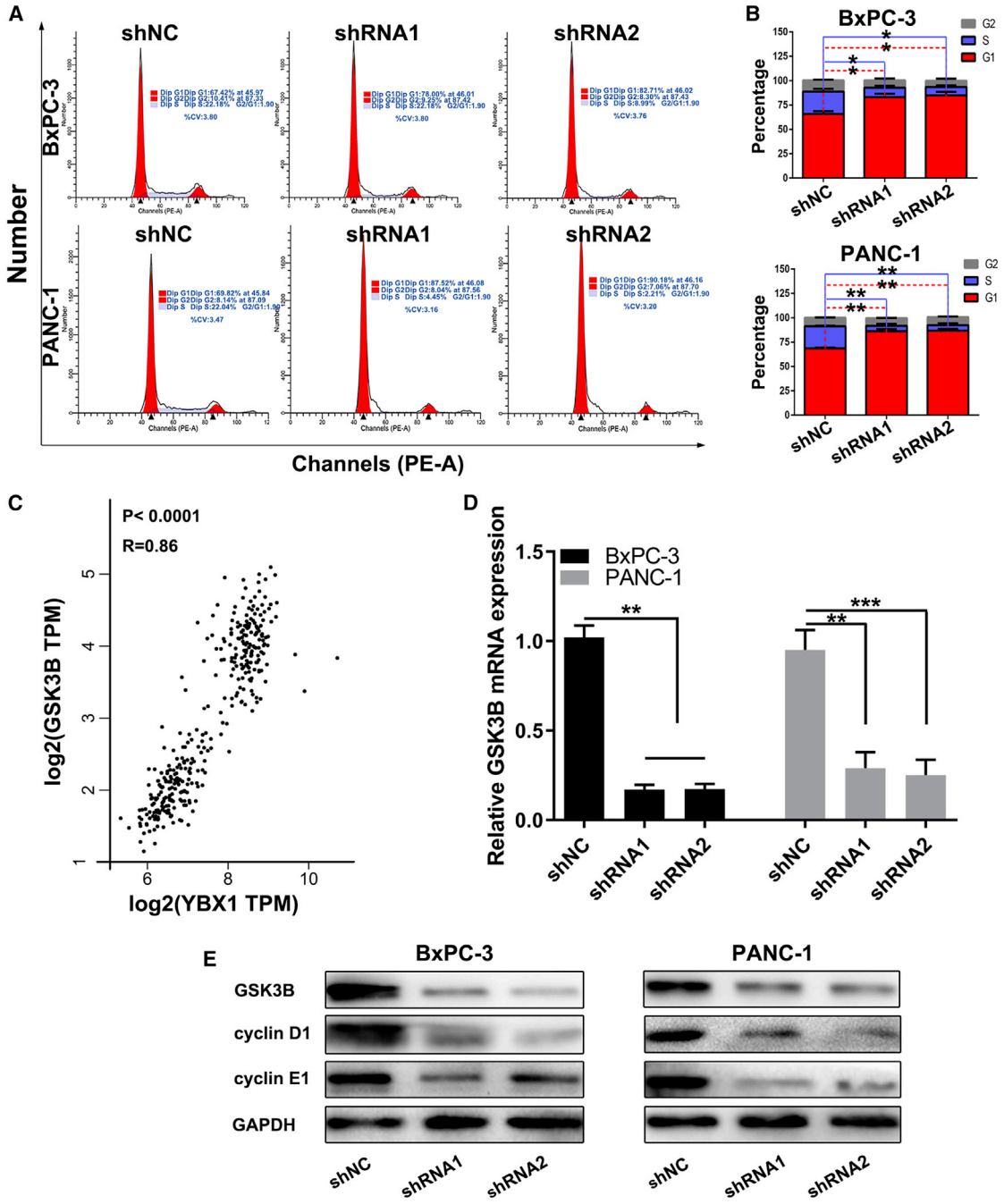

Figure 3. YBX1 Knockdown Causes Cell-Cycle Arrest and Downregulates Cell-Cycle-Related Proteins and GSK3B in PDAC Cells

(A) Silencing YBX1 in BxPC-3 and PANC-1 modulates the proportion of cells in G1 phase. Flow cytometry was used for cell-cycle analysis. The proportion in G1 phase was significantly increased, whereas in S phase it was marked decreased in YBX1 shRNA1- or shRNA2-transfected groups compared with the control group in BxPC-3 and PANC-1. (B) Statistical analysis of cell distribution in G1, S, and G2 phases in YBX1 shRNA1- or shRNA2-transfected groups compared with the control group in BxPC-3 and PANC-1. (C) *YBX1* mRNA is positively correlated with *GSK3B* mRNA. The association between *YBX1* mRNA and *GSK3B* mRNA was analyzed in GEPIA. (D) The mRNA levels of GSK3B were analyzed by polymerase chain reaction (PCR). *GSK3B* mRNA decreased in YBX1 shRNA1- or shRNA2-transfected groups compared with the control group in BxPC-3 and PANC-1. (E) Silencing YBX1 downregulates cyclin D1, cyclin E1, and GSK3B in BxPC-3 and PANC-1. Western blot was used for analyzing the protein level of GSK3B, cyclin D1, and cyclin E1. Cyclin D1, cyclin E1, and GSK3B decreased significantly in YBX1 shRNA1- or shRNA2-transfected groups compared with the control group in BxPC-3 and PANC-1. Error bars indicate standard deviation. Correlation analysis was performed using Pearson's method. The *t* test was used to compare the difference between groups. *$p < 0.05$; **$p < 0.01$; ***$p < 0.001$; ****$p < 0.0001$.

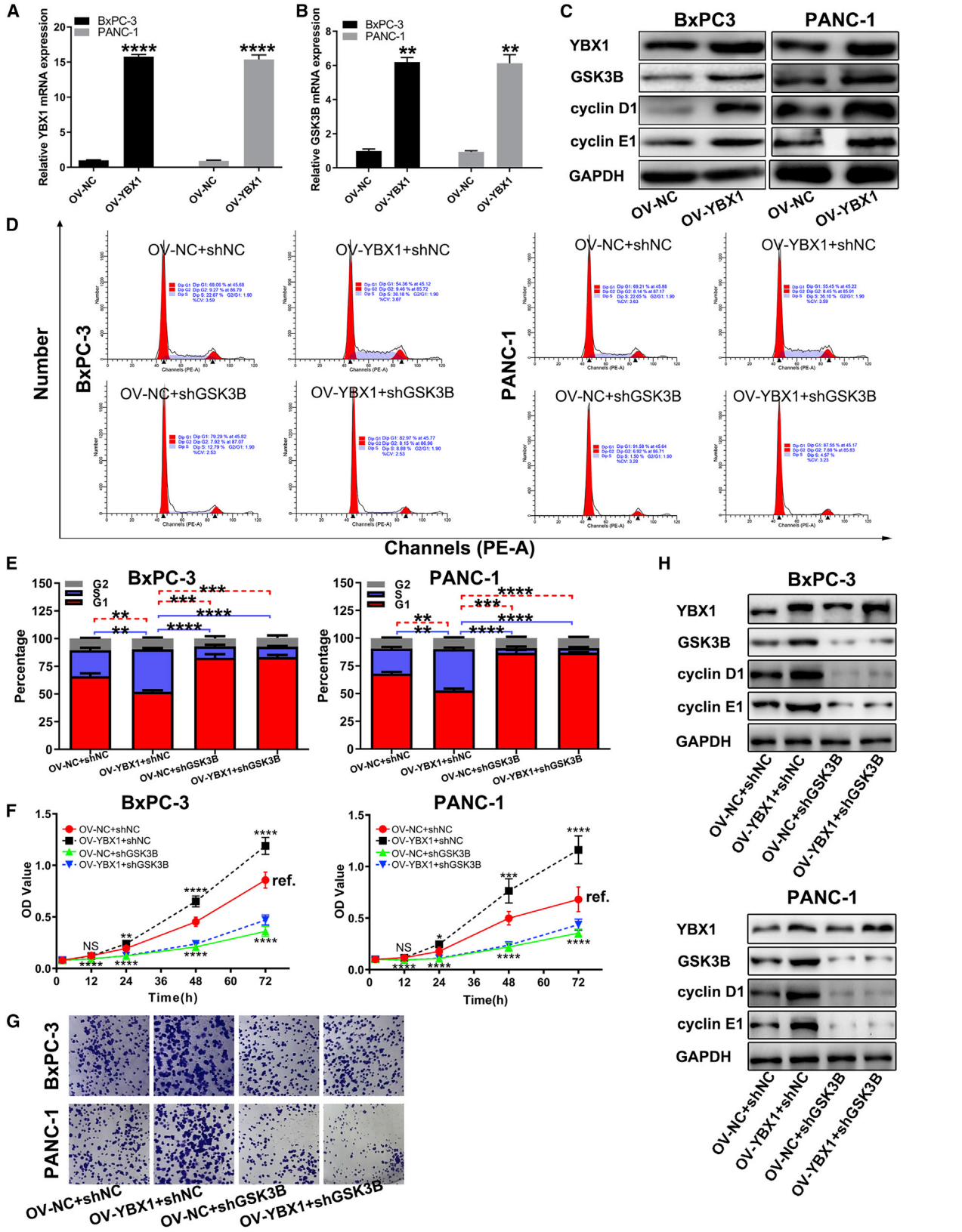

(legend on next page)

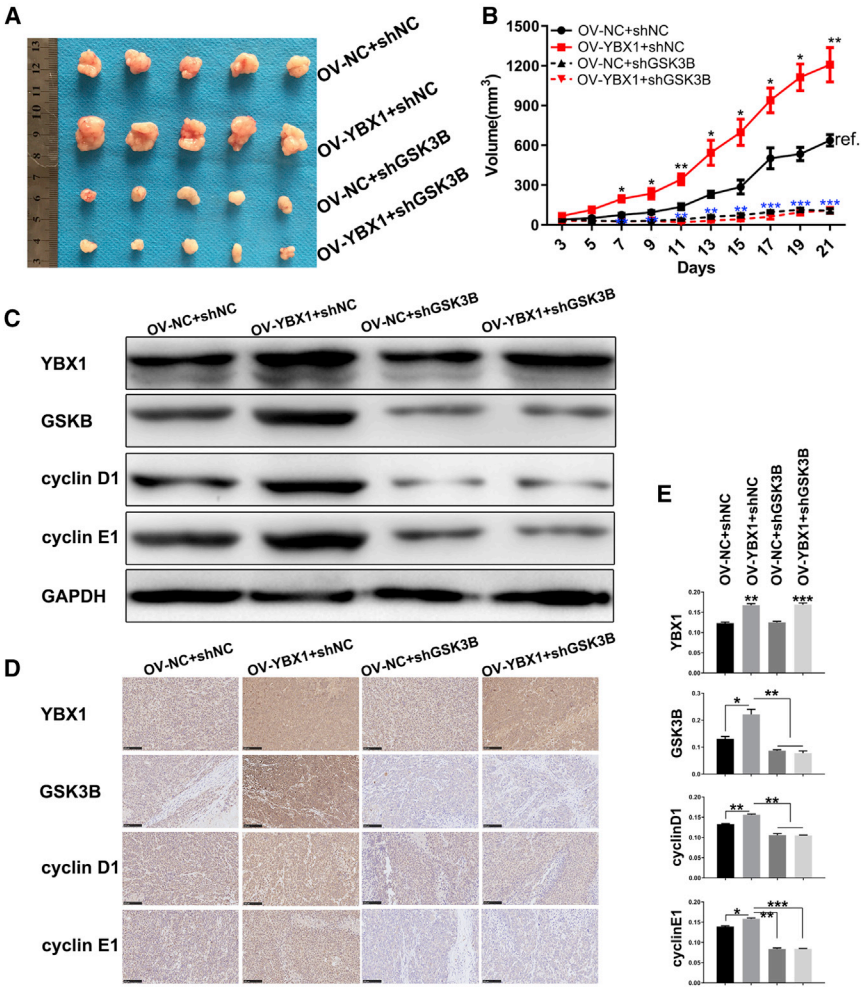

Figure 5. YBX1 Overexpression Induces Tumor Growth in Nude Mice and the Tendency Is Inhibited by GSK3B Knockdown

(A) Gross pictures of xenograft tumors 3 weeks after subcutaneous injection of BxPC-3 cells. Stably transfected BxPC-3-OV-NC+shNC, BxPC-3-OV-YBX1+-shNC, BxPC-3-OV-NC+shGSK3B, and BxPC-3-OV-YBX1+shGSK3B cells (3.0×10^6 cells) subcutaneously injected to nude mice (n = 5/group), respectively. After 3 weeks, tumors were harvested. GSK3B knockdown inhibits tumor growth *in vivo*. (B) Volume of tumors (tumor volume = length × width^2/2) obtained from xenograft models every 2 days. (C) Western blotting confirming the significantly different expression of YBX1, GSK3B, cyclin D1, and cyclin E1 in xenograft tumors between four groups of nude mice. (D) Expression of YBX1, GSK3B, cyclin D1, and cyclin E1 in xenograft tumors. (E) Statistical analysis of IHC of YBX1, GSK3B, cyclin D1, and cyclin E1 in xenograft tumors. Error bars indicate standard deviation. The *t* test was used to compare the difference between groups. *p < 0.05; **p < 0.01; ***p < 0.001; ****p < 0.0001.

YBX1 mRNA expression significantly correlates with GSK3B expression. Thus, we focused on YBX1 to investigate its roles in PDAC.

First, we showed that YBX1 is elevated in pancreatic cancer tissues compared with paired paracancer tissues (Figures 1A–1C), which corresponds with *YBX1* mRNA expression levels in PDAC versus pancreatic tissue available in GEO repositories (Figure 1D). We demonstrated that YBX1 expression correlates with poor prognosis in PDAC (Figures 1E and 1F). Western analysis showed that the expression of YBX1 protein was much higher in PDAC cell lines than that of normal pancreatic duct epithelial cell lines (Figure 1G).

To investigate the role and functional relevance of YBX1 induction in PDAC, we silenced YBX1 in PDAC cells and found that cell proliferation was significantly inhibited (Figures 2C and 2D). GSEA analysis and flow cytometry revealed that *YBX1* knockdown caused a distinct increase of cells in G1 phase and decrease in S phase (Figures 2E, 2F, 3A, and 3B). Further, correlation analysis revealed that *YBX1* mRNA levels are positively correlated with *GSK3B* mRNA levels (Figure 3C). Western analysis showed that cyclin D1, cyclin E1, and GSK3B are downregulated

Figure 4. YBX1 and GSK3B Are Both Required for Regulation of Cell-Cycle State and Proliferation

(A) BxPC-3 and PANC-1 cells were transfected with overexpression control shRNA lentiviral particle (OV-NC) or YBX1 overexpression lentiviral vectors (OV-YBX1) to increase *YBX1* gene expression. The expression levels of *YBX1* mRNA were assessed by PCR. (B) The expression levels of *YBX1* mRNA were assessed by PCR. (C) YBX1, GSK3B, Cyclin D1, and Cyclin E1 proteins were assessed by western blot analyses in BxPC-3 and PANC-1. The protein expression levels of YBX1, GSK3B, Cyclin D1, and Cyclin E1 were significantly higher in the OV-YBX1 groups compared with the OV-NC group in BxPC-3 and PANC-1. (D) Cell-cycle states were evaluated through flow cytometry. GSK3B overexpression that was induced by increased YBX1 expression increased G1 phase cell population accompanied with increased S phase cell population, and the effects could mostly be reversed by GSK3B knockdown. Cell-cycle states of BxPC-3 and PANC-1 were analyzed in OV-NC+shNC, OV-YBX1+shNC, OV-NC+shGSK3B, and OV-YBX1+shGSK3B, respectively. (E) Statistical analysis of cell distribution of BxPC-3 and PANC-1 in OV-NC+shNC, OV-YBX1+shNC, OV-NC+shGSK3B, and OV-YBX1+shGSK3B. (F) Effects of YBX1 overexpression on cell proliferation was rescued by GSK3B inhibition. CCK-8 assay was conducted in BxPC-3 and PANC-1 treated with OV-NC+shNC, OV-YBX1+shNC, OV-NC+shGSK3B, and OV-YBX1+shGSK3B, respectively. (G) Cell proliferation was assessed by colony formation in BxPC-3 and PANC-1 treated with OV-NC+shNC, OV-YBX1+shNC, OV-NC+shGSK3B, and OV-YBX1+shGSK3B, respectively. (H) The expression levels of YBX1, GSK3B, Cyclin D1, and Cyclin E1 proteins were analyzed by western blot. Error bars indicate standard deviation.The *t* test was used to compare the difference between groups. *p < 0.05; **p < 0.01; ***p < 0.001; ****p < 0.0001.

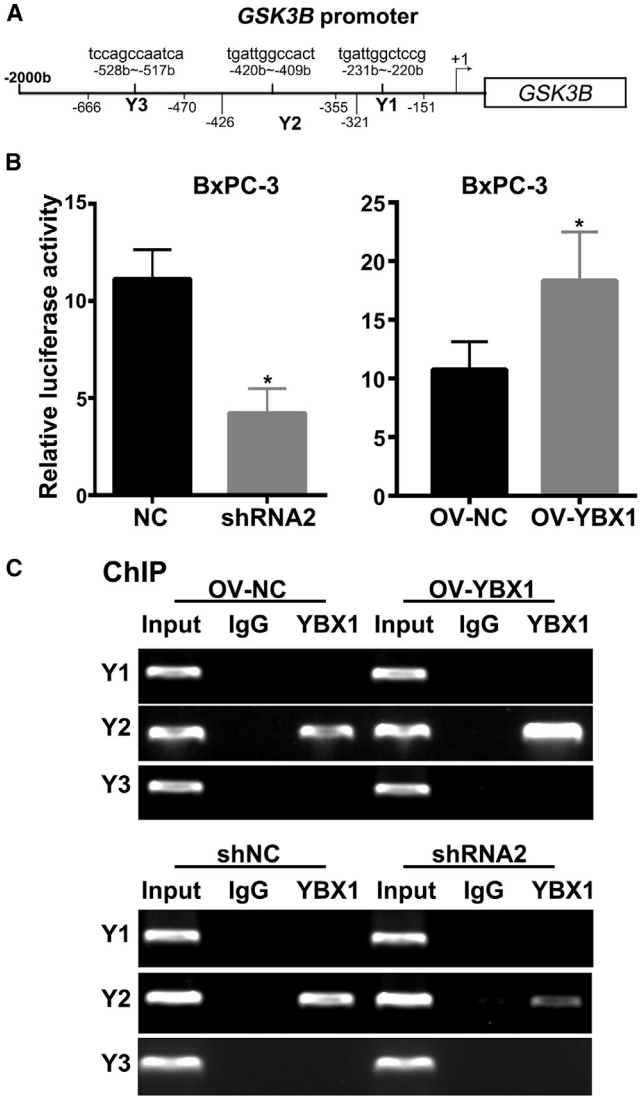

Figure 6. YBX1 Binds with the Promoter of GSK3B

(A) Schematic representation of the region (Y1–Y3) for chromatin immunoprecipitation (ChIP) in the promoter of GSK3B. Black bars show predicted YBX1 binding sites. Gray bars indicate regions for PCR primers. (B) Transcriptional activity analysis of GSK3B in BxPC-3 via dual-luciferase reporter assay system. The firefly luciferase reporter plasmid pRL-TK was transfected in inducible YBX1-ovexpression cells, cotransfected with GL3basic-control reporter in negative control cells (OV-NC), and cotransfected with GSK3B promoter in negative control cells and inducible YBX1-ovexpression cells (OV-YBX1) using Lipofectamine 2000. At 24 h, the luciferase reporter activities were assayed using the dual-luciferase reporter assay system. The luciferase activities were significantly decreased in the shRNA2 group and elevated in the OV-YBX1 group, respectively. (C) ChIP of GSK3B target gene promoters using YBX1 antibody. BxPC-3 cells were cross-linked to fix bound proteins to the DNA. Cells were lysed and the chromatin was incubated with YBX1 antibody to immunoprecipitate promoters bound by YBX1. PCR was then performed to amplify promoter fragments of known Y box genes to determine whether they were bound by YBX1. IgG, ChIP with the IgG-negative control antibody; Input, BxPC-3 DNA before immunoprecipitation; OV-NC, BxPC-3 cells transfected with overexpression control shRNA lentiviral particle; OV-YBX1, BxPC-3 cells transfected with *YBX1* gene overexpression shRNA lentiviral particle; shNC, BxPC-3 cells transfected with silencing control shRNA lentiviral particle; shRNA2, BxPC-3 cells transfected with *YBX1* gene silence shRNA lentiviral particle; YBX1, YBX1 antibody only; YBX1 ChIP, promoters immunoprecipitated with the YBX1 antibody. Error bars indicate standard deviation. The *t* test was used to compare the difference between groups. *$p < 0.05$; **$p < 0.01$; ***$p < 0.001$; ****$p < 0.0001$.

when YBX1 is silenced (Figures 3D and 3E), suggesting that GSK3B signaling may be an important effector of YBX1 signaling in PDAC. In the setting of YBX1 overexpression, opposite effects on cell proliferation, cell-cycle arrest, and related protein expression were observed compared with the YBX1 silencing groups; these effects were rescued by GSK3B knockdown *in vitro* and *in vivo* (Figures 4 and 5).

Based on these results, we explored the relationship between YBX1 and GSK3B signaling. Luciferase reporter and ChIP assays revealed that YBX1 binds directly to the promoter of *GSK3B*, regulating GSK3B expression at the transcriptional and translational levels (Figure 6). In addition, we found that *GSK3B* mRNA is significantly overexpressed in PDAC compared with normal pancreas in the GEPIA repository (Figure S1), and the *GSK3B* expression levels present in TCGA are inversely associated with overall survival and disease-free survival (Figure S1). Together, these data suggest that modulation of GSK3B may be a critical mechanism underlying the correlation between poor prognosis and high expression of YBX1 in PDAC.

In summary, this study demonstrates that YBX1 is overexpressed and correlates with poor prognosis in PDAC. YBX1 induces cell proliferation and causes cell-cycle progression through direct transcriptional activation of GSK3B expression (Figure 7). These findings offer important insights into the mechanisms underlying pathologic proliferation in PDAC.

MATERIALS AND METHODS

Pancreatic Cancer Tissues, Cell Culture, and Reagents

The experiments were undertaken with the understanding and written consent of each patient. The study methodologies conformed to the standards set by the Declaration of Helsinki. The use of human specimens for analysis was approved by the Ethics Committee of Union Hospital, Tongji Medical College, Huazhong University of Science and Technology, Wuhan, China. Pancreatic cancer tissue and adjacent noncancerous tissue samples were collected from 90 patients who had undergone surgical resection between January 1, 2012, and December 31, 2014, at Department of Pancreatic Surgery, Union Hospital, Tongji Medical College, Huazhong University of Science and Technology, Wuhan, China. Informed consent was obtained from all patients prior to surgery. Tissues were collected immediately after surgery and stored at −80°C until use.

The human pancreatic cancer cell lines BxPC-3 and PANC-1 and human pancreatic ductal epithelium cell line HPDE were purchased from Chinese Academy of Science Cell Bank (Shanghai, China) and cultured in RPMI 1640 medium (HyClone, Logan, UT, USA) with

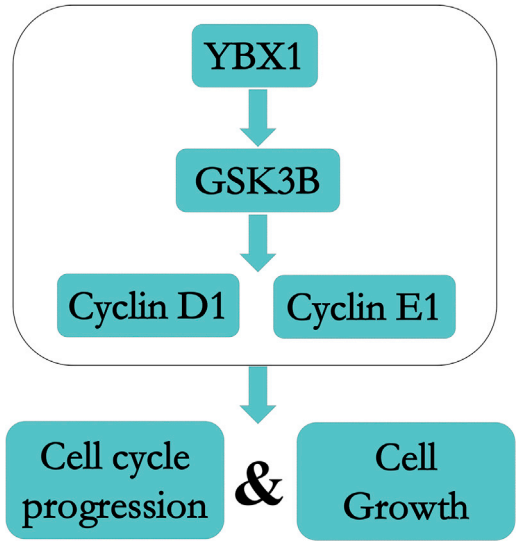

Figure 7. Models Depicting YBX1 Promote PDAC Cell-Cycle Progression and Cell Growth via the GSK3B/Cyclin D1/Cyclin E1 Pathway

10% fetal bovine serum (FBS) (ScienCell Research Laboratories, Carlsbad, CA, USA) and 1% ampicillin/streptomycin (GIBCO, San Diego, CA, USA) in a humidified incubator at 37°C with 5% CO_2. Cells were incubated in serum-free RPMI 1640 medium for 24 h before experiments.

We purchased the cell-cycle detection kit from Yeasen Biotech (Shanghai, China) and antibody against GAPDH from Proteintech Group (Wuhan, China). The following reagents were obtained from Cell Signaling Technology (Danvers, MA, USA): horseradish peroxidase-coupled secondary antibodies. Antibodies against YBX1, GSK3B, cyclin D1, and cyclin E1 were obtained from Abcam (Cambridge, UK). G418, U0126, and LY294002 were purchased from Selleck Chemicals (Houston, TX, USA). Puromycin dihydrochloride and polybrene transfection reagent were purchased from Shanghai Genechem (Shanghai, China). The research resource identifiers (RRIDs) for biological reagents used in our study are listed in Table S1.

Knockdown and Overexpression Using shRNA or shRNA Lentiviral Particles

YBX1-targeting shRNA lentiviral particles (vector control group: shNC; silencing groups: shRNA1 and shRNA2) and YBX1-overexpressing lentiviral particles (vector control group: OV-NC; overexpression group: OV-YBX1) were amplified and sequenced by Shanghai Genechem (Shanghai, China). Pancreatic cancer cells BxPC-3 and PANC-1 were transfected with *YBX1* shRNA or YBX1 overexpression lentiviral vectors to knock down or overexpress YBX1. The *YBX1* shRNAs were stably transfected into cells using a transfection reagent containing polybrene (5 μg/mL) as previously described. The control shRNA lentiviral particle, which did not target any gene, was used as a negative control. Stable clones expressing shRNAs were selected using puromycin dihydrochloride according to the manufacturer's protocol. We used *GSK3B*-targeting silencing shRNA plasmid to stably knock down GSK3B as we did before.[9]

IHC Analysis

Tissue chips and paraffin-embedded tissue sections were deparaffinized with xylene and rehydrated. The expression was assayed with antibodies against YBX1 (1:200), GSK3B (1:100), cyclin D1 (1:400), and cyclin E1 (1:100) using a similar IHC staining procedure as reported previously.[9,15] The staining intensity was classified as negative or positive by two independent reviewers.

RNA Isolation, Reverse Transcription, and qRT-PCR

Total RNA was extracted from BxPC-3 and PANC-1 pancreatic cancer cells using TRIzol reagent (Invitrogen, CA, USA) and reverse transcribed using the revers transcription kit (Takara, Dalian, China). RT-PCR and qRT-PCR were performed according to the manufacturer's protocol (Takara, Dalian, China) using an Applied Biosystems StepOne-Plus Real-Time PCR System (Thermo Fisher, Wuhan, China). mRNA levels across samples were normalized using GAPDH. Primers sequences are summarized in Table S2.

Western Analysis

Western analysis was carried out using antibodies against YBX1, GSK3B, cyclin D1, cyclin E1, and GAPDH. Cells were lysed in lysis buffer on ice for 1 h. Suspensions were centrifuged at 15,000 × *g* for 30 min at 4°C. A bovine serum albumin standard was used to quantitate protein concentrations. Equal amounts of protein were separated by sodium dodecyl sulfate-polyacrylamide gel electrophoresis and transferred onto polyvinylidene fluoride membranes (Immobilon-P; Millipore, Bedford, MA, USA). After blocking with 5% skim milk, proteins were probed with the primary antibodies and horseradish peroxidase-coupled secondary antibodies. Positive bands were detected by enhanced chemiluminescence. The results were quantified using Image Lab V.3.0 (Bio-Rad Laboratories, CA, USA).

Cell Proliferation Assay

Cell proliferation assays were conducted as previously described.[16] Cell Counting Kit-8 (CCK-8) was used according to the manufacturer's instructions. Cells were seeded into a 96-well plate and cultured in 100 μL RPMI 1640 medium supplemented with 10% FBS. At the indicated time points, the medium was exchanged for 110 μL RPMI 1640 medium with CCK-8 reagent, and the cells were incubated for 2 h. Absorbance at 450 nm was measured for each well using an auto-microplate reader.

Colony Formation Assay

To assess the capability of a single cell to grow into a colony *in vitro*, we seeded 0.1×10^4 pancreatic cancer cells in the sterile plates with complete medium. The cells were stained with 0.2% crystal violet after 2-week incubation, and the colonies were manually counted.

Cycle Analysis by Flow Cytometry

Cell-cycle analysis was performed as described previously.[17] Pancreatic cancer cells were dissociated with trypsin, suspended at 1×10^6

cells/mL, centrifuged, and washed with phosphate-buffered saline (PBS). The cells were then fixed in ice-cold 70% ethanol. The cells were resuspended in PBS with 0.1% bovine serum albumin and incubated with RNase (50 μg/mL). The cells were run on a FACSCalibur flow cytometer (BD Biosciences, CA, USA). The data were analyzed using CELL Quest software (BD Biosciences, CA, USA).

Animal Experiments

Protocols were approved by the Animal Care Committee of Tongji Medical College of Huazhong University of Science and Technology. BxPC-3 cells were stably transfected with OV-NC, OV-YBX1, OV-NC+shGSK3B, and OV-YBX1+shGSK3B. The left flank of 5-week-old male BALB/c nude mice was subcutaneously injected with the above cells for the xenograft model. Each group contained five mice. We measured tumor size every 2 days. The mice were humanely euthanized 21 days after subcutaneous injection.

Transient Transfection and Luciferase Assays

Transient transfection and luciferase assays were conducted as previously described.[18] Cells (1×10^5) were plated in six-well plates overnight prior to transfection. The cells were then co-transfected with 2 μg of the GSK3B-luc reporter construct and 0.1 μg of the Renilla luciferase-expression plasmid using 6 μL of Lipofectamine 2000. At 24 h post-transfection, the cells were lysed, and the activities of firefly and Renilla luciferases were assessed using a dual-luciferase reporter assay system.

ChIP

ChIP analysis was performed using the Millipore ChIP Assay Kit (Millipore, MA, USA) according to the manufacturer's instructions. Cells were crosslinked with formaldehyde and sonicated. Corresponding IgG was used as controls. The bound DNA fragments were subjected to PCRs using the primers in Table S1. PCR products were separated by gel electrophoresis on a 2% agarose gel.

Statistical Analysis

All data are reported as the mean ± standard deviation. The *t* test was performed to compare differences between groups. Correlation analysis was performed using Pearson's method. Kaplan-Meier curves were analyzed by log rank tests. All statistical analyses were performed using GraphPad Prism 6 software (GraphPad Software, CA, USA). Two-tailed p values <0.05 were considered statistically significant.

SUPPLEMENTAL INFORMATION

Supplemental Information can be found online at https://doi.org/10.1016/j.omto.2020.03.006.

AUTHOR CONTRIBUTIONS

H.W. and S.G. designed the experiments, and reviewed and edited the paper; Z.L., Y.L., X.L., J.Z., and S.W. conducted the experiments; Z.L. and Y.L. wrote the original draft; Z.L., X.L., J.Z., and S.W. did the data analysis; S.G. performed the funding acquisition.

CONFLICTS OF INTEREST

The authors declare no competing interests.

ACKNOWLEDGMENTS

This work was supported by grant 81472309 from the National Natural Science Foundation of China.

REFERENCES

1. Kamisawa, T., Wood, L.D., Itoi, T., and Takaori, K. (2016). Pancreatic cancer. Lancet *388*, 73–85.
2. Ryan, D.P., Hong, T.S., and Bardeesy, N. (2014). Pancreatic adenocarcinoma. N. Engl. J. Med. *371*, 2140–2141.
3. Siegel, R.L., Miller, K.D., and Jemal, A. (2017). Cancer Statistics, 2017. CA Cancer J. Clin. *67*, 7–30.
4. Tsai, S., and Evans, D.B. (2016). Therapeutic Advances in Localized Pancreatic Cancer. JAMA Surg. *151*, 862–868.
5. Lasham, A., Print, C.G., Woolley, A.G., Dunn, S.E., and Braithwaite, A.W. (2013). YB-1: oncoprotein, prognostic marker and therapeutic target? Biochem. J. *449*, 11–23.
6. Ladomery, M., and Sommerville, J. (1995). A role for Y-box proteins in cell proliferation. BioEssays *17*, 9–11.
7. Eliseeva, I.A., Kim, E.R., Guryanov, S.G., Ovchinnikov, L.P., and Lyabin, D.N. (2011). Y-box-binding protein 1 (YB-1) and its functions. Biochemistry (Mosc.) *76*, 1402–1433.
8. Lu, J., Li, X., Wang, F., Guo, Y., Huang, Y., Zhu, H., Wang, Y., Lu, Y., and Wang, Z. (2017). YB-1 expression promotes pancreatic cancer metastasis that is inhibited by microRNA-216a. Exp. Cell Res. *359*, 319–326.
9. Zhou, W., Wang, L., Gou, S.M., Wang, T.L., Zhang, M., Liu, T., and Wang, C.Y. (2012). ShRNA silencing glycogen synthase kinase-3 beta inhibits tumor growth and angiogenesis in pancreatic cancer. Cancer Lett. *316*, 178–186.
10. Tang, Z., Li, C., Kang, B., Gao, G., Li, C., and Zhang, Z. (2017). GEPIA: a web server for cancer and normal gene expression profiling and interactive analyses. Nucleic Acids Res. *45* (W1), W98–W102.
11. Didier, D.K., Schiffenbauer, J., Woulfe, S.L., Zacheis, M., and Schwartz, B.D. (1988). Characterization of the cDNA encoding a protein binding to the major histocompatibility complex class II Y box. Proc. Natl. Acad. Sci. USA *85*, 7322–7326.
12. Wolffe, A.P., Tafuri, S., Ranjan, M., and Familari, M. (1992). The Y-box factors: a family of nucleic acid binding proteins conserved from Escherichia coli to man. New Biol. *4*, 290–298.
13. Kosnopfel, C., Sinnberg, T., and Schittek, B. (2014). Y-box binding protein 1—a prognostic marker and target in tumour therapy. Eur. J. Cell Biol. *93*, 61–70.
14. Shiota, M., Izumi, H., Onitsuka, T., Miyamoto, N., Kashiwagi, E., Kidani, A., Yokomizo, A., Naito, S., and Kohno, K. (2008). Twist promotes tumor cell growth through YB-1 expression. Cancer Res. *68*, 98–105.
15. Deng, S., Zhu, S., Wang, B., Li, X., Liu, Y., Qin, Q., Gong, Q., Niu, Y., Xiang, C., Chen, J., et al. (2014). Chronic pancreatitis and pancreatic cancer demonstrate active epithelial-mesenchymal transition profile, regulated by miR-217-SIRT1 pathway. Cancer Lett. *355*, 184–191.
16. Gou, S., Cui, P., Li, X., Shi, P., Liu, T., and Wang, C. (2013). Low concentrations of metformin selectively inhibit $CD133^+$ cell proliferation in pancreatic cancer and have anticancer action. PLoS ONE *8*, e63969.
17. Fujiwara-Okada, Y., Matsumoto, Y., Fukushi, J., Setsu, N., Matsuura, S., Kamura, S., Fujiwara, T., Iida, K., Hatano, M., Nabeshima, A., et al. (2013). Y-box binding protein-1 regulates cell proliferation and is associated with clinical outcomes of osteosarcoma. Br. J. Cancer *108*, 836–847.
18. Xie, C., Liu, D., Chen, Q., Yang, C., Wang, B., and Wu, H. (2016). Soluble B7-H3 promotes the invasion and metastasis of pancreatic carcinoma cells through the TLR4/NF-κB pathway. Sci. Rep. *6*, 27528.